



# Effect of the Drying Conditions on the Microstructure of Silica Based Xerogels and Aerogels

L. Durães<sup>1</sup>, M. Ochoa<sup>1</sup>, N. Rocha<sup>2</sup>, R. Patrício<sup>2</sup>, N. Duarte<sup>3</sup>, V. Redondo<sup>3</sup>, and A. Portugal<sup>1,\*</sup>

<sup>1</sup>*CIEPQPF, Department of Chemical Engineering, University Coimbra, Pólo II, Rua Sílvio Lima, 3030-790 Coimbra, Portugal*

<sup>2</sup>*AST-Active Space Technologies, IPN-Instituto Pedro Nunes, 3030-199 Coimbra, Portugal*

<sup>3</sup>*Led and Mat, IPN-Instituto Pedro Nunes, 3030-199 Coimbra, Portugal*

Nanostructured silica based xerogels and aerogels are prepared by sol–gel technology, using methyltrimethoxysilane as precursor. The influence of the drying method and conditions on the microstructure of the obtained materials is investigated, since the drying stage has a critical influence on their porosity. Two types of drying methods were used: atmospheric pressure drying (evaporative), to produce xerogels, and supercritical fluids drying, to obtain aerogels. Although the supercritical fluids drying technique is more expensive and hazardous than the atmospheric pressure drying, it is well known that aerogels are less dense than the xerogels due to less pore shrinkage. However, the ideal situation would be to use atmospheric pressure drying in conditions that minimize the pore collapse. Therefore, in this work, different temperature cycles for atmospheric pressure drying and two heating rates for the supercritical fluids drying are tested to study the gels' shrinkage by analyzing the density and porosity properties of the final materials. The best materials obtained are aerogels dried with the lower heating rate ( $\sim 80$  °C/h), since they exhibit very low bulk density ( $\sim 50$  kg/m<sup>3</sup>), high porosity (95%)—mainly micro and mesopores, high surface area ( $\sim 500$  m<sup>2</sup>/g), moderate flexibility and a remarkable hydrophobic character ( $> 140^\circ$ ). It was proved that the temperature cycles of atmospheric pressure drying can be tuned to obtain xerogels with properties comparable to those of aerogels, having a bulk density only  $\sim 15$  kg/m<sup>3</sup> higher. All the synthesized materials fulfill the requirements for application as insulators in Space environments.

**Keywords:** Sol–Gel, Gels Drying, Nanostructures, Silica Based Materials, Space Applications.

## 1. INTRODUCTION

The bottom-up approaches to synthesize materials have experienced a significant dissemination in the last two decades, promoted by the demand of nanomaterials with improved and unique properties and supported by more powerful techniques for materials analysis at molecular scale. The sol–gel technology, applied in this work, is a good example of such trend. This technology offers many advantages over traditional synthesis methods: high purity and homogeneity of the products, low processing temperature, product microstructure control and production of advanced materials with tailored properties. Mainly, the sol–gel process starts from a homogeneous solution with a precursor that, through hydrolysis and condensation reactions, originates a colloidal solution denominated by sol. By polycondensation reactions, the sol is transformed in an integrated, and often nanostructured, solid network with the liquid phase (solvent, catalysts) in the

interstices; this semi-solid three-dimensional structure is called a gel. A xerogel or an aerogel is produced when the gel is dried at ambient pressure or in supercritical conditions, respectively.

Tetra-alkoxysilane precursors ( $\text{Si}(\text{OR})_4$ ) are widely used to obtain silica aerogels.<sup>1–3</sup> These aerogels exhibit low density ( $\sim 100$ – $350$  kg/m<sup>3</sup>), high porosity ( $> 90\%$ ) and surface area, low thermal conductivity ( $\sim 0.01$ – $0.02$  W/(m K)) and dielectric constant ( $\sim 1.1$ ), and high transparency ( $\sim 90\%$ ). These properties make them suitable for use as thermal or acoustic insulators, dielectric or optical materials, filters, catalysts, among others.<sup>1,2</sup> Despite these appealing properties, they are brittle, absorb moisture and still have a relatively high density, which might be a drawback for their performance in certain applications, namely in Space insulation applications. To make aerogels competitive with current materials for these applications, the following requirements must be met: working pressure— $10$ – $10^3$  Pa, working temperature— $150$ – $500$  °C, density— $10$ – $100$  kg/m<sup>3</sup>,

\* Author to whom correspondence should be addressed.

thermal conductivity—3–16 mW/(m K) and moderate flexibility. As far as insulation of electrical/electronic devices is concerned, the material must be hydrophobic.

Examples of relevant applications of aerogels in Space are: thermal and structural insulators for re-entry and Mars vehicles, spacecraft devices and cryogenic tanks; coatings for solar panels; semi-flexible coatings for cables, Printed Circuit Boards and Multi Layer Insulation Blankets in spacesuits and spacecrafts; collection of Space debris; acoustic insulators for spacecrafts and the International Space Station; windows and optical instruments.<sup>4</sup>

Using methyltrimethoxysilane (MTMS) precursor in a two-step acid-base catalyzed sol-gel chemistry, as proposed by Rao, Bhagat, Nadargi and co-workers,<sup>2,5-7</sup> the produced silica based xerogels and aerogels can fulfill the targets for Space applications. In trialkoxysilanes, one alkoxy group of Si(OR)<sub>4</sub> is replaced by a derivative group, for example CH<sub>3</sub> in MTMS. In this case, the methyl group does not suffer hydrolysis and remains in the gel structure after the condensation and polycondensation reactions (Fig. 1). The presence of methyl groups within the structure increases its degree of disorder and number of voids when compared to the structures obtained from tetraalkoxysilane precursors. This feature leads to an increase in porosity and consequently a reduction in density and an increase in flexibility. These methyl groups also provide high hydrophobicity to the final materials.

The key property to tailorable xerogels and aerogels for Space insulation applications is the porosity, since a high porous structure is a necessary requirement to achieve very low density and thermal conductivity. The porosity is

largely controlled by the drying technique. Although silica based xerogels and aerogels obtained from MTMS both have very low density, very high surface area and porosity, the xerogels are typically less porous and denser than aerogels. Also the drying conditions have an important effect in the porosity of the final materials and their optimization is needed to obtain materials tailored to the application.

In this work, silica based xerogels and aerogels were obtained by sol-gel technology with MTMS precursor, following the experimental procedures described by other authors<sup>2,5</sup> and also used in earlier works.<sup>8-10</sup> The implemented drying methods were atmospheric pressure drying (APD), to produce the xerogels, and supercritical fluids drying (SFD), to obtain the aerogels. Besides the drying method, the drying conditions were varied—three different temperature cycles were used in APD and two heating rates were tested in SFD—in order to evaluate the conditions that minimize the gels' shrinkage. Some works were found in the literature concerning the optimization of SFD parameters, including the heating rate,<sup>11-13</sup> but not for the case of aerogels synthesized from MTMS.

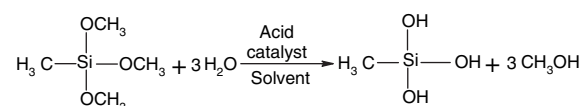
In spite of the SFD technique being known as the more effective drying method to obtain highly porous materials, it has got the disadvantages of being costly and more complex to implement than the APD. Therefore, the modification of the APD temperature cycles was done to investigate the viability for obtaining xerogels with properties close to those of aerogels, i.e., to find the conditions that minimize the pore collapse in the evaporative process.

## 2. EXPERIMENTAL DETAILS

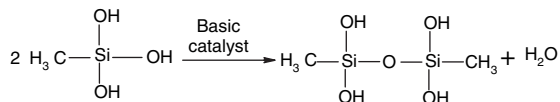
Silica based xerogels and aerogels were prepared following the sol-gel procedures described by Rao, Bhagat and co-workers<sup>2,5</sup> and previously used by the authors,<sup>8-10</sup> but making some variations on the drying conditions. MTMS (CH<sub>3</sub>Si(OCH<sub>3</sub>)<sub>3</sub>, 98%, Aldrich), methanol (CH<sub>3</sub>OH, 99.8%, Riedel-de Haën), oxalic acid (C<sub>2</sub>H<sub>2</sub>O<sub>4</sub>, 99%, Fluka) and ammonium hydroxide (NH<sub>4</sub>OH, 25% in water, Fluka) were used as precursor, solvent, acid catalyst and basic catalyst, respectively. The acid and basic catalysts were used in the form of aqueous solutions, in order to provide the water equivalents needed for the hydrolysis reaction (Fig. 1) and to control de catalysts concentrations.

A two-step acid-base catalyzed sol-gel process was applied for the synthesis of the gels. Initially, the precursor was mixed with the solvent and then the acid oxalic solution (0.01 M) was added to promote the hydrolysis reaction. After 24 h, the ammonium hydroxide solution (10 M) was joined, drop by drop, rising the pH of the solution. The alkaline conditions enhance the combination of the silanol species formed in the hydrolysis. Thus the condensation reactions occur at a faster rate, forming a sol and, some hours later (~6 h), a gel. The hydrolysis and condensation reactions were carried out at a controlled

Hydrolysis reaction:



Condensation reaction:



Polycondensation reaction :

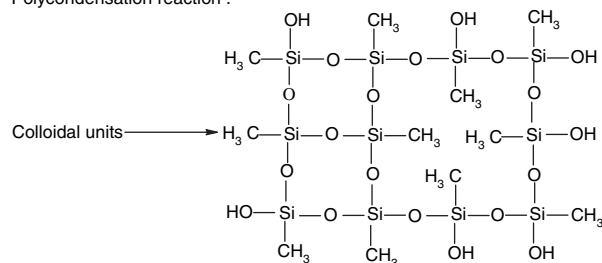


**Fig. 1.** Hydrolysis, condensation and polycondensation reactions of MTMS to give a polysilsesquioxane.

temperature of 25 °C until the completion of the addition of the basic catalyst solution. Thereafter, the gelation process occurred in a oven at a controlled temperature of 27 °C. The used molar ratios of MTMS:solvent:acidic water:basic water were 1:35:4:4. To improve the cohesion of the solid three-dimensional network, the gel was maintained at 27 °C during 2 days—aging period. Further condensation reactions, and also syneresis and cross-link coarsening processes occur during this period.<sup>3,14</sup> The molar ratios and aging period applied in this work were found to be the optimal values in earlier works<sup>2,5–8</sup> for improved properties of monolithicity, density, porosity and flexibility.

Finally, the prepared gels were dried by Ambient Pressure Drying (APD) or by Supercritical Fluids Drying (SFD) to produce xerogels and aerogels, respectively. In APD, the gels were placed in a ventilated oven, at atmospheric pressure, and submitted to several temperature cycles, as presented in Table I. To implement SFC, the gels were placed in an autoclave where the temperature was increased causing an increase in the pressure. When the critical point of the methanol solvent ( $T_c = 239.4$  °C and  $P_c = 8.09$  MPa)<sup>1</sup> was exceeded, the pressure was relieved at constant temperature ( $\sim 250$  °C). Two heating rates were tested for the increase of the autoclave temperature: 360 °C/h and 80 °C/h (Table I). The  $P$ – $T$  paths of APD and SFD processes are illustrated in Figure 2.

The temperature cycles used for Xero-a sample were the same as implemented in earlier works.<sup>5,8–10</sup> The selection of 170 °C for the last temperature step of APD in the new conditions (samples Xero-b and Xero-c) was based on the dilatometry results of the Xero-a—see Figure 3, since a contraction region above  $\sim 180$  °C was detected. Therefore, temperatures above this value were avoided to minimize shrinkage. In SFD, the higher heating rate was already used earlier<sup>8,9</sup> and the testing of a lower heating rate was decided considering the results of Rao, Pajonk and collaborators.<sup>7,11–13</sup> These authors studied the influence of this parameter in the monolithicity of silica aerogels synthesized from tetramethoxysilane (TMOS) and tetraethoxysilane (TEOS). They concluded that the best results are achieved with an intermediate heating rate. This allows a good compromise between stresses caused by pressure gradients, which increase with the heating rate,

**Table I.** Drying conditions and samples nomenclature.

Drying method	Drying conditions	Sample ID
APD	60 °C (24 h) + 100 °C (1 h) + 150 °C (1 h) + 200 °C (1 h)	Xero-a
APD	60 °C (24 h) + 100 °C (1 h) + 170 °C (2 h)	Xero-b
APD	60 °C (24 h) + 100 °C (1 h) + 170 °C (1 h)	Xero-c
SFD	Heating rate: 360 °C/h	Aero-a
SFD	Heating rate: 80 °C/h	Aero-b

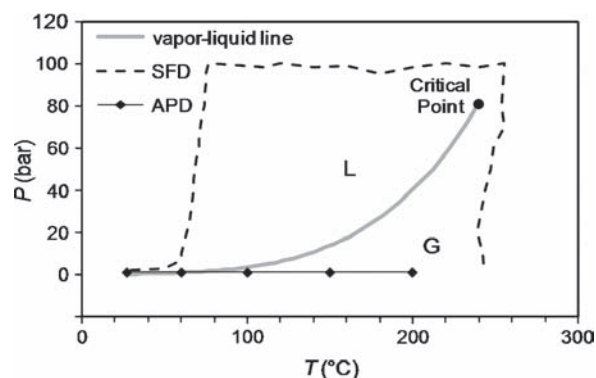


**Fig. 2.**  $P$ – $T$  paths of APD and SFD techniques: examples for Xero-a and Aero-b samples.

and the time that the gel remains at high temperatures, which decreases with increasing heating rates.

Physical, chemical, structural and thermal characterization was performed on the obtained xerogels and aerogels. The applied techniques included:

- (i) FTIR spectroscopy (FT/IR-4200, Jasco), to study the chemical structure;
- (ii) elemental analysis (EA 1108 CHNS-O, Fisons Inst.), to obtain the C, H, N and O elemental composition;
- (iii) contact angle technique (OCA 20, Dataphysics), to evaluate the hydrophobicity;
- (iv) weight and volume measurements, to calculate the apparent density;
- (v) He pycnometry (Accupyc 1330, Micromeritics), to measure the real (skeleton) density;
- (vi)  $N_2$  gas adsorption (ASAP 2000, Micromeritics), to obtain the surface area and the pore size distribution;
- (vii) scanning electron microscopy—SEM (JMS-5310; JOEL), to observe the microstructure;
- (viii) DSC/TG (PL-STA 1500 H, Rheometric Scientific), to study the thermal behavior and stability;

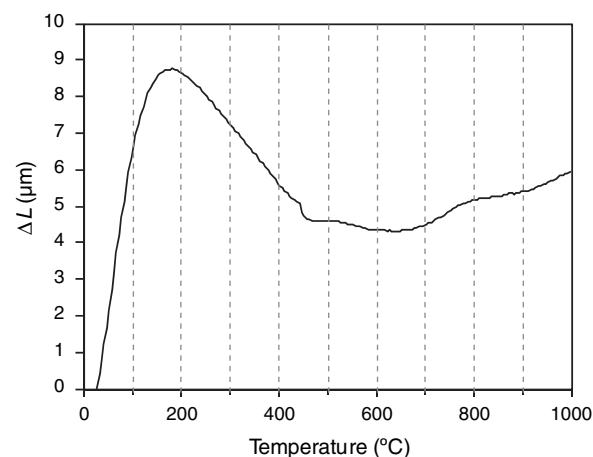


**Fig. 3.** Dilatometry curve for Xero-a.

(ix) dilatometry (Differential Dilatometer 402 ED, NET-ZSCH), to evaluate the expansion and contraction of the materials as a function of temperature.

### 3. RESULTS AND DISCUSSION

All the obtained materials were flexible monoliths with the shape of the test tubes, as shown in Figure 4.

During the addition of the basic catalyst solution—basic step of the synthesis, a sharp pH increase (from  $\sim 2.5$  up to  $\sim 9.5$ ) was observed with the addition of the first two drops ( $\sim 0.1 \text{ cm}^3$ ); then, the pH increased slowly towards its final value (pH  $\sim 11$ )—Figure 5. It was observed that more intense condensation started with the beginning of the basic catalyst addition since the solution became slightly cloudy, proving that a strong effect was achieved with a tiny amount of catalyst. Thus, the alkaline medium favors the condensation reactions, fact in agreement with the literature.<sup>3,14</sup>

The FTIR spectra obtained for all the synthesized xerogels and aerogels were similar, showing that the chemical structure of the materials is independent of the drying method and conditions. Typical FTIR results for the xerogels and aerogels are presented in Figure 6. The assignment of the peaks was based on data for similar systems.<sup>15</sup> The observed vibration bands confirm the expected chemical structure for these materials (see also Fig. 1): a predominant inorganic network based on Si–O–Si bonds



Fig. 4. Photograph showing the typical appearance of the synthesized monoliths of xerogels and aerogels.

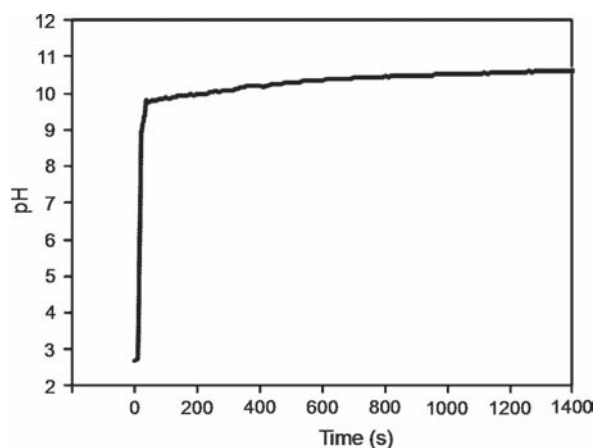


Fig. 5. Record of the pH evolution during the basic step of the syntheses.

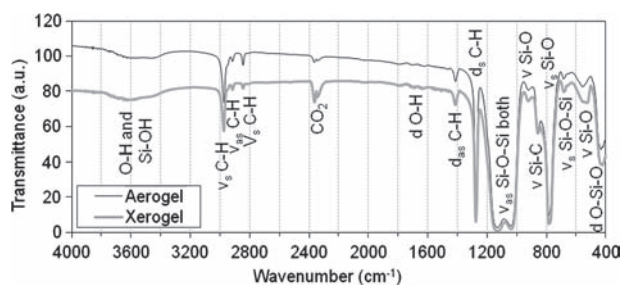


Fig. 6. Typical FTIR spectra for the prepared silica based xerogels and aerogels ( $\nu$ —stretching vibration;  $d$ —bending vibration;  $s$ —symmetric;  $as$ —asymmetric).

(silica), with a methyl group per Si (hybrid materials) and –OH terminal groups at the network ends.

The elemental analysis results and the contact angle values obtained for all the synthesized materials are summarized in Table II. The theoretical elemental ratios calculated for complete condensation hypothesis, neglecting the OH groups at the structure ends, are 1Si:1C:3H:1.5O and 41.8Si:17.9C:4.5H:35.8O in molar and wt% base, respectively. For the case of no condensation of one OH group of the silanol (monomer), these ratios are 1Si:1C:4H:2O and 36.9Si:15.8C:5.3H:42.0O. The theoretical and experimental values of wt% C are the most adequate to be compared in order to evaluate the extent of the condensation/polycondensation reactions, since the values of wt% H and wt% O are significantly and cumulatively affected by several factors, such as:

- (i) residues of solvent and catalysts in the samples;
- (ii) the OH terminal groups of the solid network were not considered in the calculus;
- (iii) the temperature used in the elemental analysis furnace (1060 °C) is not enough to break the Si–O bonds.

The first point is corroborated by the no null experimental values found for the wt% N ( $\sim 0.3$ – $0.4$ ), which are surely due to basic catalyst residues. The second item is an unavoidable limitation resulting from not knowing the number of OH groups at the structure ends. The item (iii) is the reason for the excessively low experimental values of wt% O (2.6–3.5) found for all the samples.

The experimental values of wt% C are in better agreement with the theoretical hypothesis of complete condensation (Table II) that leads to a wt% C of 17.9.

Table II. Elemental analysis results for C, H, O and N and contact angle values for the synthesized xerogels and aerogels.

Sample	wt% C <sup>(a)</sup>	wt% H <sup>(a)</sup>	wt% O <sup>(a)</sup>	wt% N <sup>(a)</sup>	Contact angle (°)
Xero-a	19.145	4.992	2.956	0.426	136.3 ± 4.6
Xero-b	18.481	5.341	2.653	0.326	147.5 ± 4.5
Xero-c	18.811	5.121	2.679	0.433	140.5 ± 11.3
Aero-a	19.212	5.094	3.101	0.388	138.7 ± 10.8
Aero-b	19.602	5.122	3.467	0.362	146.6 ± 3.0

Note: <sup>(a)</sup>The wt% errors associated with the measurements are  $\pm 0.43$ ,  $\pm 0.20$ ,  $\pm 0.15$  and  $\pm 0.25$  and for C, H, O and N, respectively.

The obtained contact angles do not show significant differences between the samples (Table II), what was expected since the wt% C values do not also vary much. A contact angle of  $\sim 140^\circ$ , as was obtained, is characteristic of highly hydrophobic materials.

The already discussed results show that the chemical structure of the produced materials is quite independent of the drying method. Then the physical features of the xerogels and aerogels will be analyzed.

Table III presents the bulk and skeleton densities and the porosity estimated considering these values, for all the produced materials. The materials with lower bulk density are the aerogels dried with a heating rate of  $80^\circ\text{C/h}$  and the xerogels dried with  $170^\circ\text{C}$  (1 h) in the last temperature step, being the best aerogels less dense than xerogels, as expected. Thus, the SFD appears to be the most suitable technique when materials of tight porosity specifications are required, although it is more expensive and hazardous than the APD. However, when the APD cycles are properly adjusted, the final materials can have a bulk density very close to that of aerogels, in this case only  $\sim 15\text{ kg/m}^3$  higher. The differences observed in the skeleton density values may be due to different amounts of closed pores and/or lightweight impurities. These variations naturally affect the porosity estimates that could be more sensitive to the bulk density if the former were absent.

The specific surface areas and the average pore sizes of the synthesized materials were obtained using the nitrogen adsorption/desorption isotherms (Fig. 7) and considering the BET and BJH models, respectively, and are presented in Table III. It can be observed that the surface area of xerogels is very high— $\sim 400\text{ m}^2/\text{g}$ , but the surface area of Aero-b is even higher— $\sim 500\text{ m}^2/\text{g}$ . Aero-a sample has a lower surface area, what can be explained by its significantly higher bulk density. The surface area values of the xerogels and aerogels are globally in agreement with their bulk density and porosity values. The very high surface area exhibited by these materials make them also suitable for surface-dependent applications.

The synthesized materials have an average pore size of  $33\text{--}44\text{ \AA}$  (Table III) that is included in the size interval of mesopores, but it is close to the boundary between micropores and mesopores ( $20\text{ \AA}$ ). In fact, the obtained adsorption/desorption isotherms show typical

**Table III.** Bulk and skeleton densities, porosities, surface areas and pore sizes of the synthesized materials.

Sample	Bulk density (kg/m <sup>3</sup> )	Skeleton density (kg/m <sup>3</sup> )	Porosity (%)	BET surface area (m <sup>2</sup> /g)	BJH desorption pore size (Å)
Xero-a	$78.4 \pm 10.5$	1133.6	93.1	$426.5 \pm 10.6$	36
Xero-b	$78.9 \pm 10.7$	1284.4	93.9	$437.4 \pm 9.2$	38
Xero-c	$70.1 \pm 3.1$	1112.5	93.7	$416.7 \pm 10.9$	33
Aero-a	$97.2 \pm 19.7$	1183.6	91.8	$232.0 \pm 5.4$	37
Aero-b	$53.6 \pm 6.1$	1154.5	95.4	$512.4 \pm 11.0$	44

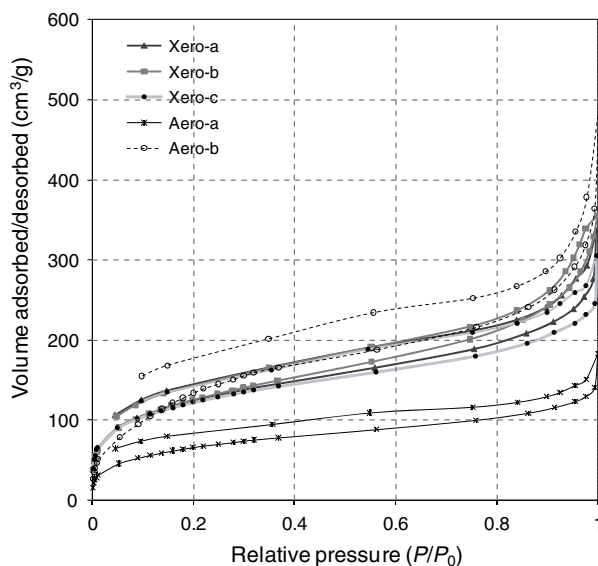


**Fig. 7.** Nitrogen adsorption/desorption isotherms of the synthesized xerogels and aerogels. The upper branch of each curve corresponds to the desorption stage.

profiles of mesoporous materials (type IV isotherms)—Figure 7, although the pore size distribution curves—Figure 8—show also an increment of pore volume for pore sizes below  $20\text{ \AA}$  (it should be noted that the nitrogen gas adsorption technique only allows the quantification of pores down to  $\sim 15\text{ \AA}$ ). Therefore, it can be concluded that the synthesized materials have a significant volume of either micropores and mesopores, thus being microporous and mesoporous materials. Consistently with the bulk density results, the registered adsorbed and pore volumes (Figs. 7 and 8) for Aero-b are the highest and the contrary occurs for Aero-a.

SEM images for the studied materials are presented in Figure 9. Similar cloudy and diffuse structures, with very small interlinked units (much smaller than  $1\text{ }\mu\text{m}$ ), are observed for all the produced materials. In general, the structural patterns are very ramified, which is consistent with the low bulk density and the presence of a large

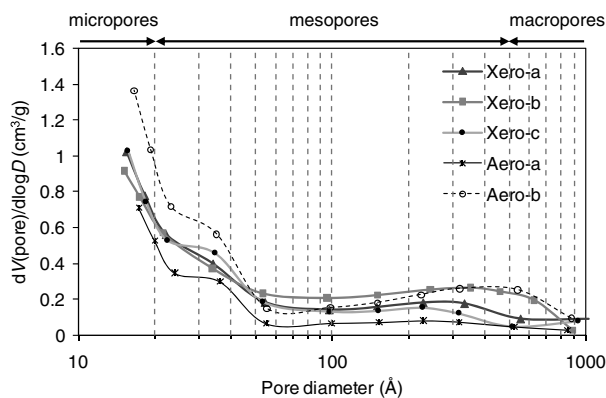


**Fig. 8.** Pore size distributions obtained by nitrogen desorption for all the produced samples.

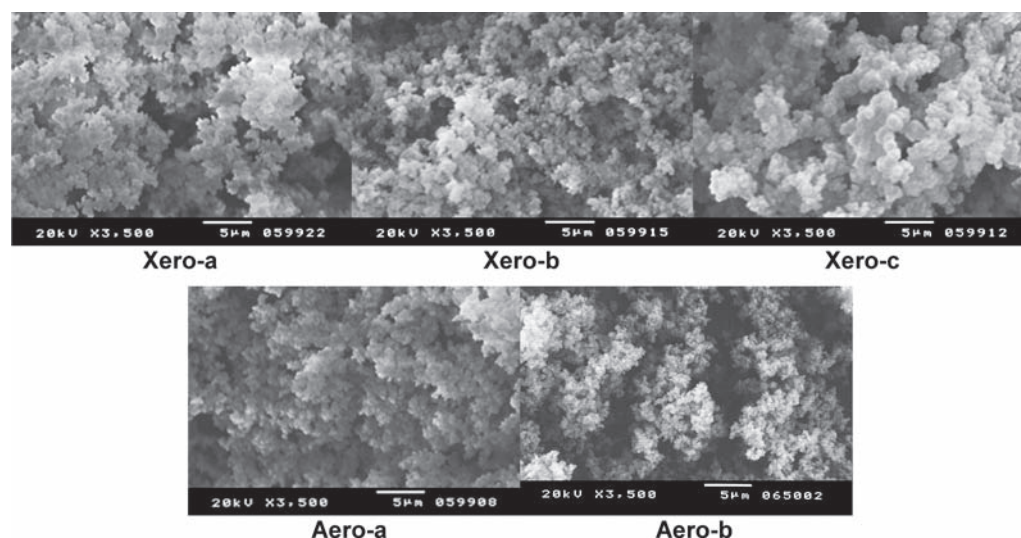


Fig. 9. SEM micrographs of the synthesized materials.

amount of pores in the materials. As expected, denser materials show more closed patterns (see, for example, Aero-a). The materials with lower bulk density—Xero-c and Aero-b—have large holes in their structures (macropores). The effect observed in an earlier work<sup>9</sup> (where the acid catalyst solution concentration was 0.001 M) of larger interlinked units for evaporative drying is only slightly observed with the current conditions for Xero-c.

A SEM micrograph of Aero-b with higher magnification can be observed in Figure 10. It is noticeable that the interlinked structural units have a nanometric size. In addition, besides the pores of micrometric size already observed in the lower magnification micrograph, pores much smaller than 1  $\mu\text{m}$  are visible in Figure 10 between the interlinked units, which are certainly the micro and mesopores detected by the nitrogen gas adsorption technique.

In Figure 11, a typical result of the thermal analysis of the xerogels and aerogels is presented. The materials do not suffer any thermal changes up to 300  $^{\circ}\text{C}$  and preserve their integrity up to  $\sim 800$   $^{\circ}\text{C}$ . The first weight loss

( $\sim 2.5\%$ ) starts at  $\sim 300$   $^{\circ}\text{C}$  and is due to the reaction and release of residual organic compounds<sup>5</sup> (ex.: catalysts) or/and to the loss of some OH terminals. This small loss is an exothermic phenomenon, corresponding to the small and wide hump in the DSC curve between 300 and 450  $^{\circ}\text{C}$ . The next two sharp and intense exothermic peaks, with maxima at 540  $^{\circ}\text{C}$  and 625  $^{\circ}\text{C}$  are due to the methyl groups oxidation.<sup>5,16</sup> Thus, the thermal stability of Si–C bonds is preserved up to  $\sim 500$   $^{\circ}\text{C}$ , where the first of these two peaks begins. The two step oxidation of methyl groups is accompanied by a weight loss of approximately 10%. This phenomenon develops in two stages, since it was used a  $\text{N}_2$  atmosphere for the analysis and, consequently, the  $\text{CH}_3$  oxidation was only accomplished by the residual oxygen inside the system. The material becomes hydrophilic as a result of the Si–C bond oxidation into Si–OH, being the OH group responsible for the adsorption of water.<sup>5,16</sup>

Finally, upon a preliminary test at low pressures, it was concluded that the synthesized materials remain unchanged after being exposed to high vacuum (1 Pa).

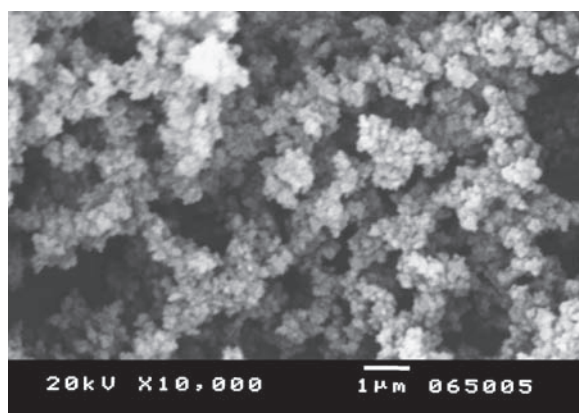


Fig. 10. SEM micrograph of Aero-b with higher magnification.

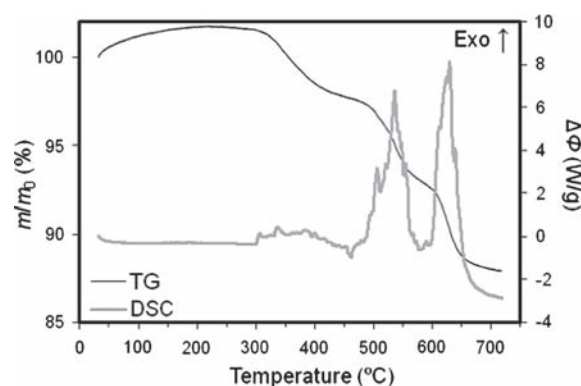


Fig. 11. Typical TG and DSC curves obtained in a nitrogen atmosphere (heating rate—10  $^{\circ}\text{C}/\text{min}$ ) for the synthesized materials.

#### 4. CONCLUSIONS

The sol-gel technology was applied to produce silica based xerogels and aerogels, using MTMS as precursor. The influence of the drying method and conditions on the chemical, physical and structural features of the obtained materials was investigated. The drying methods were atmospheric pressure drying (APD), to produce the xerogels, and supercritical fluids drying (SFD), to obtain the aerogels. Three different temperature cycles were tested in APD, while two heating rates were experimented in SFD.

It was concluded that the drying method and conditions do not have an observable influence on the chemical structure/composition of the synthesized materials, but the drying stage has a significant influence on their bulk density. SFD is the most appropriate drying technique to obtain products (aerogels) with the lowest density (highest porosity), suitable for insulation purposes in Space. The best aerogels were dried with a low heating rate (80 °C/h) and have the following properties: very low density ( $\sim 50 \text{ kg/m}^3$ ), high porosity (95%), high surface area ( $\sim 500 \text{ m}^2/\text{g}$ ), small pore size ( $\sim 40 \text{ \AA}$ ), moderate flexibility, high hydrophobic character ( $> 140^\circ$ ) and good thermal stability. It was also proved that the APD temperature cycles can be tuned to obtain xerogels with properties similar to those of aerogels, having a bulk density only  $\sim 15 \text{ kg/m}^3$  higher.

All the synthesized materials—xerogels and aerogels—fulfill the requirements for application in the form of insulator layers for Space devices, as they have a density lower than  $100 \text{ kg/m}^3$ , a work temperature up to  $500 \text{ }^\circ\text{C}$ , a work pressure down to  $1 \text{ Pa}$ , moderate flexibility and high hydrophobicity.

**Acknowledgments:** This work was developed under the project “AerTPS - Aerogel Thermal Protection Systems” by the Consortium “AST/FCTUC/IPN,” funded by QREN, under the Operational Program for Competitiveness Factors granted by the European Regional Development Fund.

#### References and Notes

1. A. C. Pierre and G. M. Pajonk, *Chem. Rev.* 102, 4243 (2002).
2. A. V. Rao, S. D. Bhagat, H. Hirashim, and G. M. Pajonk, *J. Colloid Interface Sci.* 300, 279 (2006).
3. A. Soleimani Dorcheh and M. H. Abbasi, *J. Mater. Process. Technol.* 19, 10 (2008).
4. J. Hernández and R. Patricio, ESA Type A contract no.19528/NL/06/CO, Active Space Technologies (2008).
5. S. D. Bhagat, C.-S. Oh, Y.-H. Kim, Y.-S. Ahn, and J.-G. Yeo, *Microporous Mesoporous Mater.* 100, 350 (2007).
6. N. D. Hedge and A. V. Rao, *J. Mater. Sci.* 42, 6965 (2007).
7. D. Nadargi, S. Latthe, and A. Rao, *J. Sol-Gel Sci. Technol.* 49, 53 (2009).
8. L. Durães, S. Nogueira, A. Santos, C. Preciso, J. Hernandez, and A. Portugal, *Proc. 10th Int. Chem. Biol. Eng. Conf.—CHEMPOR 2008*, edited by, E. Ferreira and M. Mota, Department Biological Engineering, University of Minho, Braga (2008), p. 563 and CD-ROM.
9. L. Durães, M. Ochoa, A. Portugal, N. Duarte, J. P. Dias, N. Rocha, and J. Hernandez, *Adv. Sci. Technol.* 63, 41 (2010).
10. M. Ochoa, L. Durães, A. Matos Beja, and A. Portugal, *Mater. Res. Bull.* (2011), under review.
11. G. M. Pajonk, A. V. Rao, N. N. Parvathy, and E. Elaloui, *J. Mater. Sci.* 31, 5683 (1996).
12. G. M. Pajonk, A. V. Rao, B. M. Sawant, and N. N. Parvathy, *J. Non-Cryst. Solids* 209, 40 (1997).
13. A. V. Rao, D. Haranath, G. M. Pajonk, and P. B. Wagh, *Mater. Sci. Technol.* 14, 1194 (1998).
14. C. J. Brinker and G. W. Scherer, *Sol-Gel Science*, Academic Press, Boston (1990).
15. R. Al. Oweini and H. El-Rassy, *J. Mol. Struct.* 919, 140 (2009).
16. A. V. Rao, M. M. Kulkarni, D. P. Amalnerkar, and T. Seth, *J. Non-Cryst. Solids* 330, 187 (2003).

Received: xx Xxxx xxxx. Accepted: xx Xxxx xxxx.